Electronic structure of $LiBeH_3$

M. R. Press, B. K. Rao, and P. Jena
Physics Department, Virginia Commonwealth University, Richmond, Virginia 23284-2000
(Received 6 November 1987)

Using a molecular-cluster representation, we have studied the equilibrium lattice spacing and the electronic structure of $LiBeH_3$. The former was obtained by minimizing the total Hartree-Fock energies of a number of clusters consisting of up to 15 atoms in a simple cubic as well as a modified perovskite structure. The resulting lattice constant is found to be in fair agreement with the value obtained by Overhauser from an analysis of the powder-diffraction data. The electronic structure of the hydride was investigated by calculating the partial and total density of states, electron-charge density distribution, and ionic character of the constituent atoms in clusters of up to 27 atoms using the local-density-functional theory. The lack of a prominent structure in the density of states at the Fermi energy and the evidence of directional bonding from the electron density map imply that $LiBeH_3$ does not have as much metallic character as previously expected. Thus, the system may not be a high-temperature superconductor *if* dependent upon conventional mechanisms. The density of states of $LiBeH_3$, on the other hand, bears a strong resemblance to those of the new high-T_c materials.

I. INTRODUCTION

The search for materials exhibiting superconductivity at high temperatures has been going on for a much longer period than the current events[1] may appear to indicate. Metallic hydrogen, due to its light mass and high electron density, has been predicted[2] to be a high-temperature superconductor with the predicted transition temperatures ranging between 140 and 260 K. Since hydrogenation also makes some otherwise normal metals superconducting,[3] Overhauser recently examined[4] the possibility that lithium beryllium hydride may exhibit high-temperature superconductivity. He began by analyzing the Debye-Scherrer powder-diffraction patterns obtained by Bell and Coates[5] nearly 20 years ago. The ten powder-diffraction lines Overhauser observed are the first ten allowed reflections of an fcc translation group. He proposed a tentative modified perovskite structure for $LiBeH_3$ as shown in Fig. 1. This differs from the simple-cubic perovskite structure in the sense that the occupancy of the cube centers and corners alternate between Li and Be. Such a chemical superstructure is consistent with the odd, odd, odd Bragg reflections observed experimentally.[5] The corresponding lattice constant predicted[4] for this modified perovskite is 5.09 Å.

The assignment of this structure and the corresponding lattice constant brings out some striking features. For example, the total atomic concentration of $LiBeH_3$ would exceed that of diamond by a factor of 1.7 and the conduction electron density would correspond to the density parameter $r_s = 1.64a_0$, which is typically in the range assumed for metallic hydrogen. Thus, if one could show that $LiBeH_3$ is metallic, it may exhibit superconductivity at high temperatures. This would be particularly interesting since $LiBeH_3$ is stable at ordinary pressure and temperature and hydrogen does not desorb from it until about 300 °C.

This optimism, however, rests on several factors: (i) The predicted lattice constant of 5.09 Å implies that the shortest distance between two hydrogen atoms in this light-mass hydride has to be 1.8 Å. This is smaller than the "magic" distance of 2.1 Å which Switendick[6] observed empirically between two nearest hydrogen atoms from a survey of all existing stable metal hydrides. Thus, if the predicted lattice constant of $LiBeH_3$ is true,

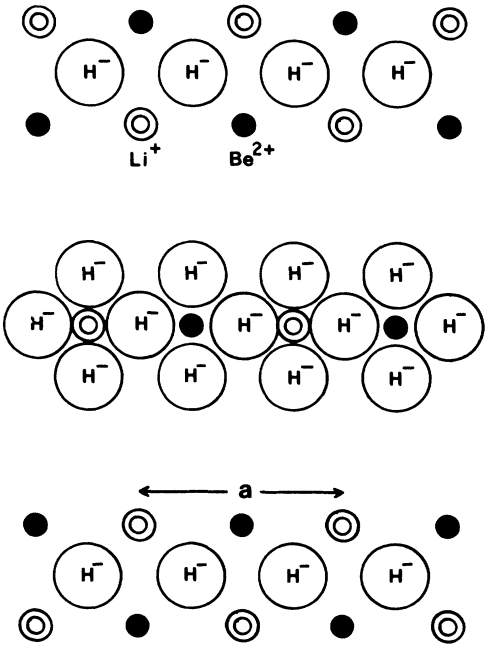

FIG. 1. Schematic diagram of three atomic layers of $LiBeH_3$ as proposed by Overhauser (Ref. 4).

it would be the first stable hydride to deviate from the Switendick criterion.[7] On the other hand, if the lattice constant of $LiBeH_3$ would be larger, say, by a factor of 2 or $\sqrt{2}$ than what is predicted, the corresponding conduction electron density would be much smaller than that in metallic hydrogen. Thus the hope of high-temperature superconductivity would diminish even if the system is found to be metallic. (ii) As observed by Overhauser, the perovskite structure favors divalent (positive) ions at cube centers and monovalent (positive) ions at cube corners. The chemical superstructure proposed in Fig. 1 does not conform to this rule. To be consistent the crystal needs to exhibit nonionic character. (iii) A significant density of states at the Fermi energy as well as a delocalized nature of electron density distribution would be among the desirable features for a hydride were it to exhibit metallic behavior.

In order to address these issues, we have carried out self-consistent electronic structure calculations of $LiBeH_3$ by approximating the infinite solid by a small cluster of atoms confined to both the simple-cubic and modified perovskite structure. Two different but complementary sets of calculations are performed to obtain the equilibrium lattice constant, atomization energy, electron charge density distribution and density of states. The total energy calculations were performed on small-size clusters using an unrestricted Hartree-Fock (UHF) approximation[8] and a Gaussian representation of the atomic basis functions.[9] This scheme allows an accurate determination of the total energy which can be minimized to obtain the equilibrium lattice constant. The electron density of states were determined by considering large clusters embedded in an effective medium that simulates the periodic solid. We have used the local density functional (LDF) theory[10] for this latter set of calculations. Finally, the electron density maps obtained from both UHF and LDF methods are compared to understand the role of correlation and the adequacy of the LDF approximation.

In Sec. II we briefly outline our theoretical procedure. The results are discussed in Sec. III and a summary of our conclusions are presented in Sec. IV.

II. THEORETICAL PROCEDURE

We have used a molecular cluster approach to study the electronic structure of periodic solids. Here one represents the solid by a finite cluster of atoms. Such an approach is relevant in situations where (i) the interactions are governed by the local environment, (ii) enough atoms are used in the cluster such that the computed properties are not size dependent, and/or (iii) the symmetry of the solid is low enough that conventional band-structure methods are difficult. For the modified perovskite structure shown in Fig. 1, conventional band calculations are time consuming. Further, it will be prohibitively expensive if one were to allow further structural distortion due to hydrogen motion. In our cluster calculation we have used clusters consisting of up to 27 atoms that are confined to lattice locations given in Fig. 1 as well as in simple-cubic perovskite structure. Some of the clusters are also embedded in an effective medium that simulates the periodic environment. Such a procedure minimizes the effect of the cluster surface on calculated bulk properties and also enhances the self-consistency procedure.

Our calculations are based upon a self-consistent-field–linear combination of atomic orbitals–molecular orbital (SCF-LCAO-MO) method.[8,11] The MO eigenstates $\psi_n(\mathbf{r})$ are expanded in terms of symmetry orbitals $\chi_j(\mathbf{r})$,

$$\psi_n(\mathbf{r})=\sum_j C_{nj}\chi_j(\mathbf{r}) . \tag{1}$$

The $\chi_j(\mathbf{r})$ are themselves chosen as linear combinations of atomic orbitals centered on different atoms corresponding to the cluster point-group symmetry. In two different calculations, we represent atomic functions in terms of Gaussian and numerical basis sets, respectively. The former allows one to evaluate the energy matrix elements analytically, thus providing a more accurate determination of the total energy. The latter, however, has the advantage that one avoids ambiguities associated with fitting wave functions to a limited number of Gaussian orbitals. These problems will become more apparent as we discuss our results in the next section.

The coefficients C_{nj} in Eq. (1) are obtained variationally by solving the single-particle equation,

$$(H-\varepsilon_n)\psi_n(\mathbf{r})=0 . \tag{2}$$

The effective Hamiltonian for a state of spin σ is given in Hartree units by

$$H=-\frac{\nabla^2}{2}+V_{\text{Coul}}+V^{\sigma}_{\text{ex}}+V^{\sigma}_{\text{corr}} . \tag{3}$$

The various terms in Eqs. (2) and (3) carry their conventional meaning. For the determination of the equilibrium lattice constant, we have ignored the effect of correlation potential, V_{corr}, and have treated the exchange potential V^{σ}_{ex} within the unrestricted Hartree-Fock approximation. The neglect of correlation does not affect the interatomic distance. The reader is referred to a recent article by Rao and Jena[12] for more details of the numerical procedure.

The remaining calculations are done by applying the local density approximation to the exchange and correlation potential in Eq. (3). We have used the von Barth-Hedin[13] form of the spin-dependent potential for this purpose. The single-particle equations (2) are solved using the discrete variational method[11] (DVM) where one minimizes certain error moments on a diophantine sampling grid in $\mathbf{r}$,

$$\langle\chi_i \mid H-\varepsilon \mid \psi\rangle=0 . \tag{4}$$

The matrix secular equation $(\mathbf{H}\text{-}E\mathbf{S})\mathbf{C}=0$, where $\mathbf{H}$ and $\mathbf{S}$ are the Hamiltonian and overlap matrices, respectively, is solved by standard procedures to yield coefficients C_{nj} and discrete energy eigenvalues E_n. The lowest-energy MO's are filled successively with cluster electrons up to a self-consistently determined Fermi energy invoking Fermi-Dirac statistics. The cluster charge density is constructed by summing over all MO's with occupation

$f_n(\varepsilon)$:

$$\rho_{\text{cluster}} = \sum_n f_n \mid \psi_n(\mathbf{r}) \mid^2 . \tag{5}$$

To calculate the potential by one-dimensional integrations, this charge density is recast in a multicenter-overlapping multipolar form,

$$\rho_{\text{model}}(\mathbf{r}) = \sum_{lm} d^j_{lm}(n)\rho_j(\mathbf{r}_n)Y_{lm}(\hat{r}_n) , \tag{6}$$

with $\mathbf{r}_n = \mathbf{r} - \mathbf{R}_n$. The radial density basis set $\{\rho_j\}$ is composed of spherical atomic densities where the atomic orbitals are obtained by solving the free-atom problem. Each atom species is provided with $1s$, $2s$, and $2p$ orbitals. Attractive spherical wells are added to the atomic potentials as to reduce overlap between orbitals on different atomic sites without significantly affecting diffuse conduction electron states or distorting the core orbitals, a step which is known to produce an improved variational basis. This near-minimal set is further augmented with five parabolic radial functions for all $l \leq 1$ in the fully symmetric representation of the molecular point group. This additional variational freedom is imperative in view of the very dense packing of atoms (metal-hydrogen distance $= 1.27$ Å) in the lattice, since addition of further virtual unoccupied atomic orbitals proves to be unfruitful. The need for an extensive treatment of basis functions in a densely packed solid will become apparent when we discuss the UHF results of the ionicities of constituent atoms obtained from a near-minimal and split-valence basis.

In simulating the bulk solid from a finite cluster of atoms, each of these clusters is embedded in the effective crystal potential field constructed by placing atomic/ionic potentials at all appropriate lattice sites out to a distance of 15 a.u. By making the peripheral atoms in the cluster sense a potential and charge density closer to that of the bulk, this scheme accelerates convergence of such properties as the density of states and the electron charge distribution. An Ewald summation of the potential over unit cells is employed to ensure the correct Madelung potential.

III. RESULTS AND DISCUSSIONS

The clusters employed for the lattice-constant determination in the UHF calculation are shown in Fig. 2.

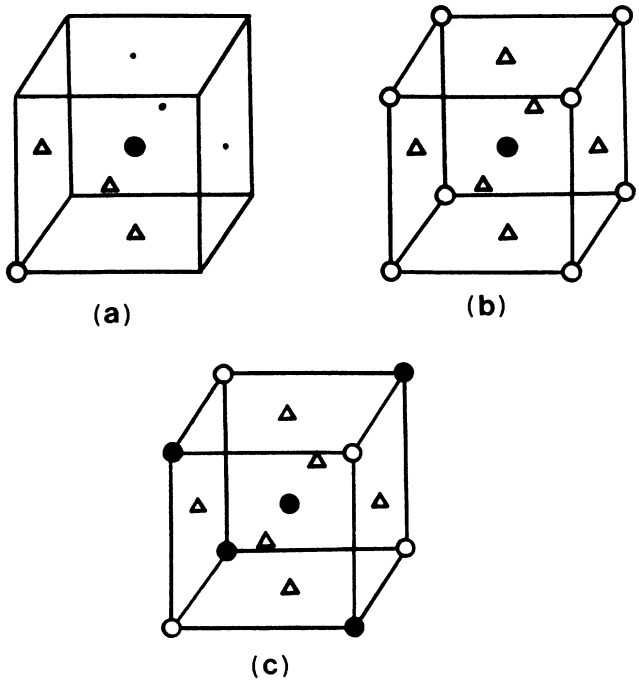

FIG. 2. Geometries of the clusters studied using the SCF-LCAO-MO Hartree-Fock method. The occupied positions on the cubic lattice are represented by solid circles (Be), open circles (Li), and triangles (H).

Figure 2(a) represents a minimal $LiBeH_3$ cluster that preserves the perovskite structure. It, however, cannot distinguish between the simple-cubic and the modified structure proposed by Overhauser in Fig. 1. Figure 2(b) and 2(c) correspond, respectively, to atomic arrangements in the simple-cubic and modified perovskite phases. The equilibrium lattice constants were obtained by minimizing the total energies as a function of interatomic distance. For each cluster we have calculated the total energies obtained using the split-valence (6-31G) basis functions[9] for $1s$, $2s$, $2p$ orbitals of Li, Be, and H. To emphasize the need of an extended basis set such as the splitting of the valence functions, we have also used a modified basis set where Li atoms are represented by STO-6G basis and the other atoms are left unchanged. The resulting equilibrium distances obtained from the minimum in the total energy for the clusters are compared in Table I.

TABLE I. Unrestricted Hartree-Fock results for the geometries shown in Fig. 2.

Geometry	a_{opt} (Å)	E_{HF} (Hartree)	Atomization energy (eV)	Mulliken population Be (center)	Be (corner)	Li	H
Fig. 2(a)	5.59	−23.728 749	6.421	3.568		2.529	1.301
Fig. 2(b)	6.07	−77.492 637	13.235	3.316		2.758	1.437
Fig. 2(c)	5.97	−106.065 685	14.076	2.708	3.911	2.744	1.445
Fig. 2(a) (modified basis)	5.69	−23.694 504	6.341	3.766		2.418	1.272
Fig. 2(b) (modified basis)	5.74	−77.372 992	16.793	2.030		2.988	1.511

Several observations can now be made: (1) The equilibrium lattice constant in the simple-cubic and modified perovskite structures are nearly the same. (2) Comparison of lattice constants determined from clusters in Figs. 2(a) and (b) indicate an expansion of the lattice as clusters grow. This is typically what is seen in metallic clusters[7] and the interatomic distances are known to saturate to their bulk value for rather small-sized clusters. Thus, our calculated value of the lattice constant in Fig. 2(c) should be very close to the bulk value. Note that our value is 17% higher than that determined by Overhauser. The effect of correlation tends to reduce the interatomic distance,[7] although this effect is typically less than 5%. To eliminate the possibility that this discrepancy of 17% could be due to inaccuracy in our calculations, we compare the equilibrium lattice constants of LiH crystal and equilibrium bond length of LiH molecule also calculated within the HF approximation with experimental values. Our results[14] for these are 7.3 and 3.0 a.u., respectively, which agrees very well with the experimental values of 7.6 and 3.014 a.u. Thus, the explanation for the discrepancy may lie in one of the following. The superstructure used by Overhauser may not be the correct one. A more likely reason, however, may be related to the large zero-point motion of hydrogen which may cause the surrounding atoms to relax outward. This would give rise to an expanded lattice bringing Overhauser's value to closer agreement with ours. It is also interesting to note that our predicted value of 2.1 Å distance between the two nearest H atoms is in agreement with the empirical observation of Switendick.[6] (3) The atomization energy (defined as the energy gained by breaking up the cluster into individual atoms) for the modified perovskite structure Fig. 2(c) is higher than that for the simple-cubic phase, thus tending to prefer the former structure over the latter. (4) We have studied a modified perovskite structure where the central atom in Fig. 2(c) is replaced by Li. The computed lattice constant of 5.96 Å is nearly identical to that in Fig. 2(c). (5) The results obtained using the modified basis (STO-6G for Li and 6-31G for Be and H) provide lattice constants in good agreement with those obtained using extended basis. However, the predicted ionicities of the central Be atom [Fig. 2(b)] are quite different. This clearly points to the need for using a good basis function for the study of electronic structure. (6) The charge on the atoms determined from a Mulliken population analysis in Fig. 2(c) indicates that hydrogen is anionic with a charge of -0.45. This is consistent with the behavior of H in all metallic systems. The Li and Be corner atoms are nearly neutral indicating that their participation in chemical bonding is substantially less than those at the center. On the other hand, the central Be is strongly cationic. A charge-density analysis to follow will show that the central atoms bond strongly with hydrogen through a charge-transfer mechanism.

Since the correlation affects electronic properties more than the lattice spacing, we have performed the following electronic structure calculations using the LDF method. In these calculations, we have used the empirically determined lattice constant of 5.09 Å. Our results for the electronic structure are, however, not very sensitive to small changes in the lattice constant.

We note from Fig. 1, that there are two distinctly coordinated sets of Li and Be atoms in the proposed $LiBeH_3$ lattice. One set occupies alternate cube centers and the other occupies alternate cube corners, while all the face centers of the cubes with side a are occupied by hydrogen. We shall call these sets Li(1) and Li(2), and Be(1) and Be(2), respectively. Type-(1) atoms are at a distance of $(a/4)$ from the nearest H while type-(2) atoms are at a distance of $(a/4)\sqrt{2}$. The following clusters pictured in Fig. 3 have been chosen for our study.

(a) 21-atom clusters $LiLi_4Be_4H_6Be_6$ and $BeBe_4Li_4H_6Li_6$, having T_d symmetry, and composed of a central Li(1) or Be(1) atom and all its nearest neighbors up to a distance of $a/2$ [see Fig. 3(a)].

(b) 27-atom clusters $LiLi_4Be_4H_{12}Be_6$ and $BeBe_4Li_4H_{12}Li_6$, having T_d symmetry, and composed of a central Li(2) or Be(2) atom and its nearest neighbors up to a distance of $a/2$ [Fig. 3(b)].

(c) A 25-atom cluster $LiBeHH_2H_8Li_4Li_2Be_4Be_2$, with C_{2v} symmetry, composed of all atoms encasing two perovskite cubes of side $a/2$ placed atop each other [Fig. 3(c)].

The above nonmenclature of the clusters is to emphasize

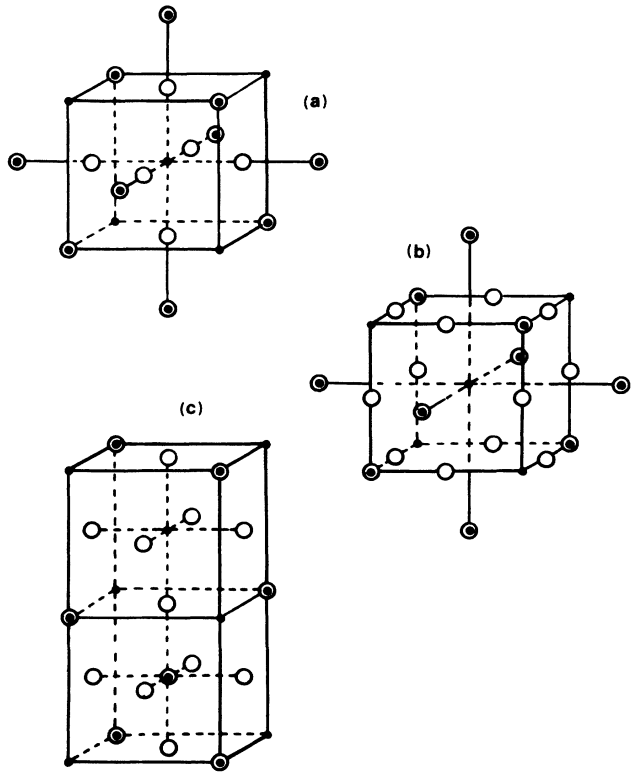

FIG. 3. Geometries of (a) 21-, (b) 27-, and (c) 25-atom clusters studied using LDF-DVM. The open circles represent H atoms. The solid circles and the double circles represent Be and Li atoms (or alternatively Li and Be atoms), respectively. The lattice constant is 5.09 Å, as given by Overhauser.

the fact that the various subsets of like atoms are treated as distinct from each other for electron charge density and potential analysis. Due to the boundary conditions of the cluster-medium interaction, one expects the central region of a cluster having atomic sites with full or close-to-full coordination to be best described. Thus, the rationale behind choosing the size and composition of clusters is to ensure full coordination to the Li, Be, and H atoms in the center of the cluster.

We shall now correlate the cluster density of states and the charge-density analysis from the various cluster calculations. Total density of states (TDOS) for majority spins in $LiBeH_3$ and site-projected local density of states (LDOS) at Li(1), Li(2), Be(1), Be(2), and H sites are displayed in the sequence of Figs. 4(b), 5(a), 5(b), 6(a), 6(b), and 4(a), respectively. This will not only be useful for the following discussion of the nature of electronic states, but may be compared with x-ray photoemission and ultraviolet photoemission spectra when available. The discrete cluster eigenvalues have been smeared out using Lorentzians to simulate solid-state bands. Since all the net spin densities are uniformly $\leq \pm 0.05$, the majority spin DOS have not been shown. While the DOS arising from a finite-cluster calculation may not be as accurate as those derived from band-structure calculations, their broad features can provide a qualitative description of the electronic structure. The structure in Fig. 4(b) at 9–10 eV is predominantly of s character. Both Be(1) and Be(2) show peak structure about 6–7 eV below the Fermi energy corresponding to a strong sp^3 hybridization between Be $2p$ and H $1s$ levels, with a little Li(1) $2p$ contribution. The structure peaking around 1.5–2.0 eV is due to the overlap between the p states of nearest neighbor Li and Be.

To obtain TDOS to the same accuracy as the LDOS, one needs a cluster where all the type-(1) and type-(2), as well as H atoms, are well represented in terms of their local coordination shell. Such a cluster would be computationally prohibitive. Consequently, the TDOS given here is obtained not from a particular cluster calculation, but from an addition of LDOS for Li(1) + Li(2) + Be(1) + Be(2) + 6H corresponding to a unit cell $Li_2Be_2H_6$.

In order to see how well this TDOS may represent a real system. we have performed calculations on a 25-atom cluster [Fig. 3(c)]. This cluster has Li(1), Be(1), and H atoms well represented. Our calculations for this cluster give virtually the same distribution of energy levels for its three atoms as obtained above. Also, using a half-ionic basis set (i.e., ionic atomic basis sets corresponding to + 0.5 charge on Li, + 1.0 on Be, and −0.5 on H) results in an upward shift of ≈ 1 eV in all DOS structure near the Fermi energy. This is consistent with the compressed nature of the cationic orbitals.

Each of the LDOS decomposed according to site represents the central atoms in the 21- and 27-atom clusters. This becomes necessary since the effect of incomplete bonding and dangling bonds, which the peripheral cluster atoms are subject to in spite of the embedding scheme, is more dramatic for this very compact system and serves to push the spectrum of DOS levels attributed to these atoms up by about 1–2 eV. The contribution to the peak at 2 eV in the LDOS for hydrogen [Fig. 4(a)] comes from the overlap of hydrogen s and p orbitals with the peripheral cluster atom orbitals.

The Fermi energy (defined to be at $E=0$ in Figs. 4–6) lies in the valley beyond the uppermost valence band. There is very little contribution ($< 10\%$ of the peak) to the DOS at the E_F and very little structure in the conduction band. The first set of antibonding states appear 5 eV above the Fermi energy. This lack of structure in DOS at the Fermi energy is not typical in systems that exhibit metallic behavior.[15] The structure of the total density of states, however, resembles strongly[16] those found in the newly discovered high-T_c materials.

The electronic structure can also be studied by analyzing the charge density in terms of the Mulliken population and volume charges. Although charge transfer and ionicities are not obtained from legitimate commuting quantum-mechanical operators, these two quantities, in spite of being qualitative and subject to particular methods of measurement, do retain chemical significance. It is possible to detect certain trends in the ionicities which are independent of the positioning of a site within a cluster, or the type of atomic/ionic orbital basis used, allowing us to make generalized statements about site-projected ionic charges. For example, the ionic charge on H is consistently between −0.4 and −0.5; that on Li(1) is 0.5–0.70; on Li(2) it is 0.20–0.40, and on both

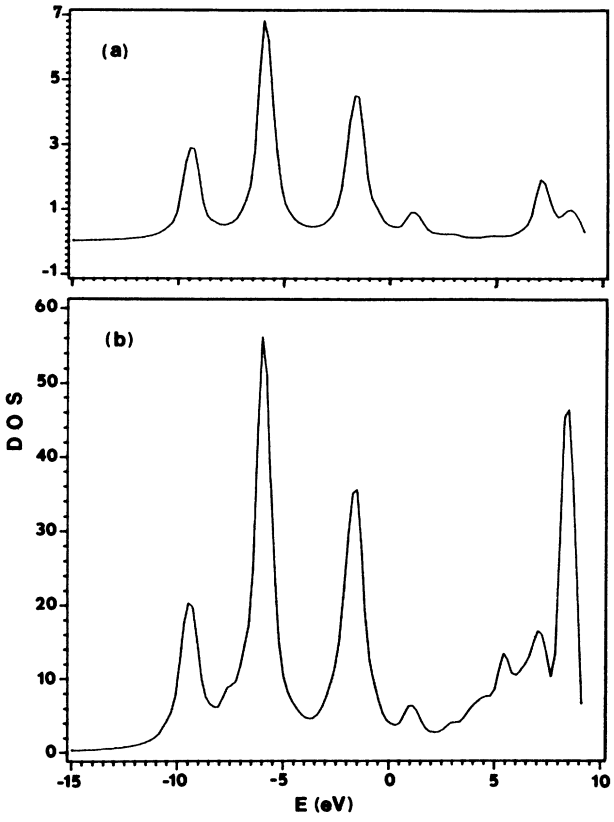

FIG. 4. (a) Local density of states at hydrogen atom sites. (b) Total density of states. The Fermi energy is placed at $E=0$.

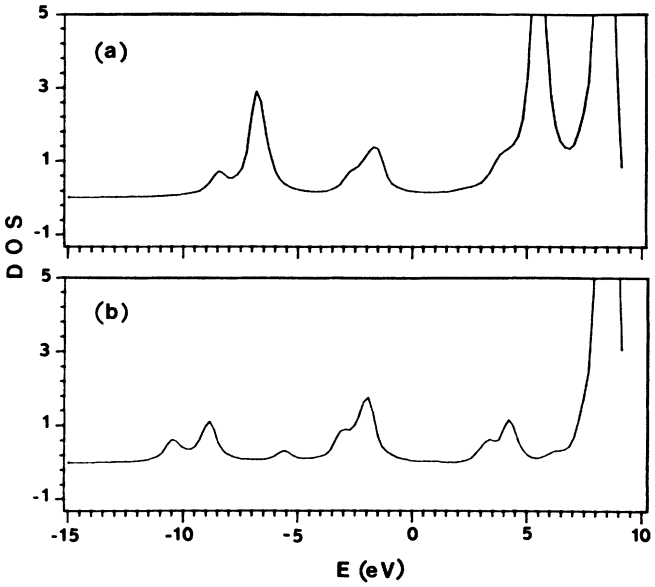

FIG. 5. Local density of states at lithium atoms situated at (a) Li(1), (b) Li(2). Note that the peaks after the Fermi energy (placed at $E=0$) have been truncated to highlight low-lying states.

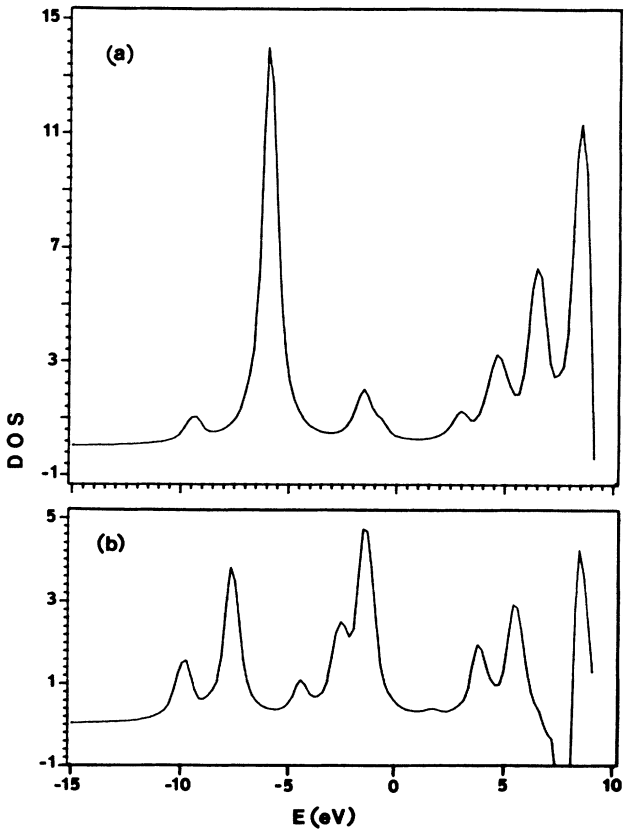

FIG. 6. Local density of states at beryllium atoms situated at (a) Be(1), (b) Be(2). The Fermi energy is placed at $E=0$.

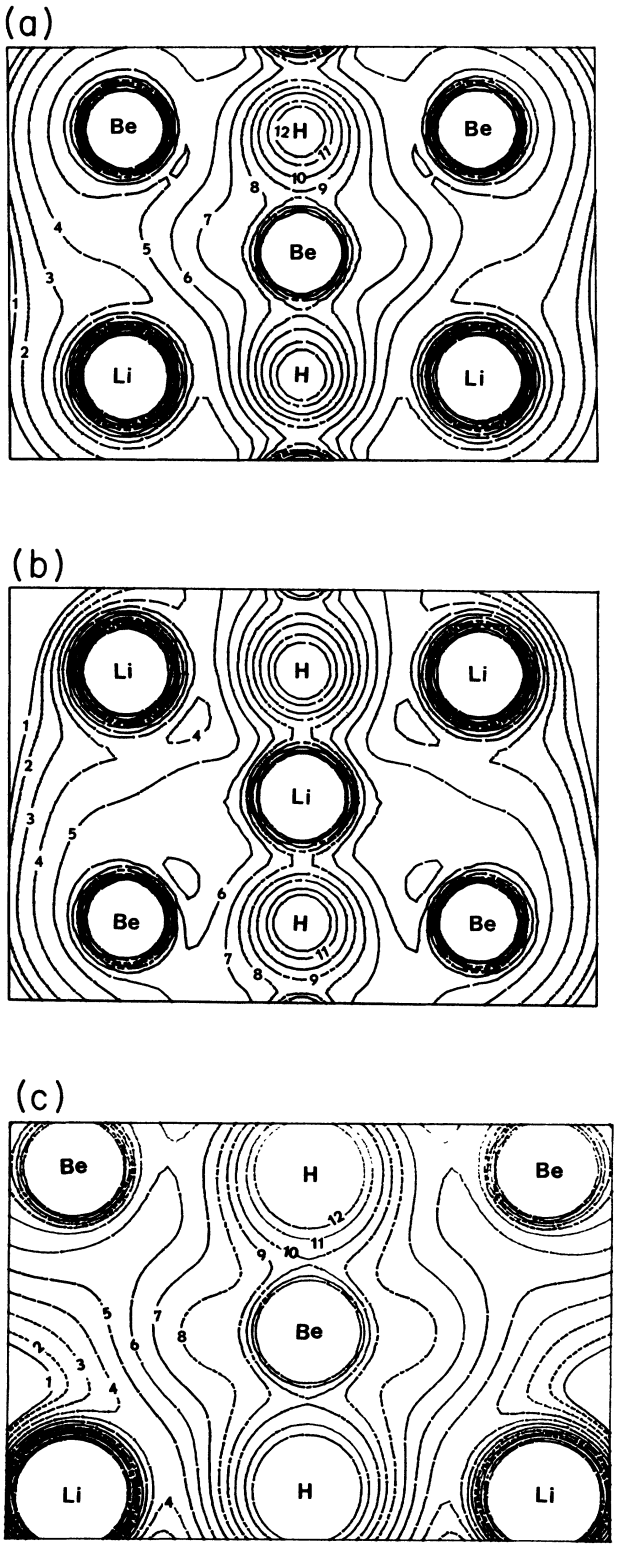

FIG. 7. (a) DVM charge density contour along the (110) plane of a cube of $LiBeH_3$ with Be at body center. The inset numbers 1–12 represent the values of 0.005, 0.006, 0.008, 0.011, 0.015, 0.020, 0.026, 0.033, 0.041, 0.050, 0.065, and 0.080 a.u., respectively. (b) Same as (a) but with Li at center. (c) Charge-density contour for the same geometry as in (a) obtained by the UHF technique.

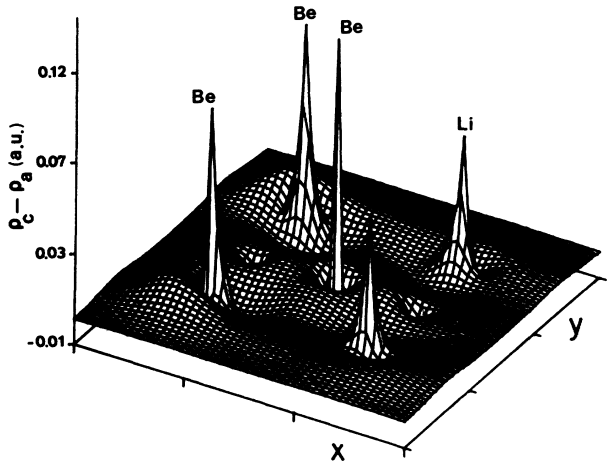

FIG. 8. LDF-DVM difference charge density (cluster-free atom) corresponding to Fig. 7(a).

types of Be between 1.0 and 1.3. These results on ionicities agree well with the UHF results presented in Table I and discussed earlier.

In Figs. 7(a) and 7(b), we plot the charge-density contours in the (110) plane arising from the 21-atom clusters in Fig. 3(a). Figure 7(a) corresponds to the cluster with Be at the center while Fig. 7(b) is for the cluster with Li at the center. These charge densities are based upon the LDF calculations. Note that the contours around the corner metal atoms are nearly spherical, indicating a weak bond between Li(2) and Be(2) with hydrogen. This trend is also reflected in the Mulliken charge analysis discussed earlier. On the other hand, the strong bonding of the central Li and Be atoms with neighboring hydrogen is apparent. This produces a chainlike corrider for electron conduction while the surrounding atoms/ions serve to stabilize the linkage. In Fig. 7(c) we plot the UHF charge-density contours in the identical format as that in Fig. 7(a). The strong similarity between the charge-density distributions obtained from UHF and LDF calculations provide additional confidence on our electronic structure results on $LiBeH_3$.

To illustrate the effect of self-consistent interaction of electrons on their distribution, we plot in Fig. 8 the difference charge densities. It is obtained by subtracting from the SCF-LDF results charge densities constructed from a superposition of atomic densities. The strong anionic character of H atoms is clearly visible from the pileup of charge in the bonding direction between central Be and H.

IV. CONCLUSIONS

Self-consistent calculations of the equilibrium lattice constants and electronic structure of $LiBeH_3$ have been carried out by using a molecular cluster representation. The theoretical procedures involved both unrestricted Hartree-Fock and local density approximation to the density functional methods. Several conclusions can be made: (1) The calculated lattice constant is in fair agreement with that determined by Overhauser. While the lattice constants are not sensitive to the choice of atomic basis functions, the electronic structure is. (2) The bonding of hydrogen with metal atoms distinguishes between atoms located at cube corners and centers. While the cube-corner atoms remain close to neutral, the strong charge transfer between the central metal atoms and hydrogen gives rise to a stable covalent bond. This result is independent of the approximations in the exchange and correlation potential. (3) The density of states is dominated by the Be ($2p$) and H ($1s$) bonding. It does not have much structure near the Fermi energy and differs from those commonly found in the metallic systems. (4) The electronic structure does not provide enough enthausiasim for believing that $LiBeH_3$ may be a "poor man's metallic hydrogen" under conventional superconductivity mechanisms. However, its density of states bears strong resemblance[15] to those in high T_c ceramic materials. In addition, the chemical bonding is directed from central metal atoms to H. Thus, the possibility of unconventional superconductivity mechanisms may make further study of $LiBeH_3$ worthwhile.

ACKNOWLEDGMENTS

This work was supported in part by the Department of Energy under Contract No. DE-FG05-87ER45316. We are also thankful to Professor A. W. Overhauser for sending us a copy of his work prior to publication.

[1]A. Khurana, Phys. Today, **40**(4), 17 (1987).

[2]N. W. Ashcroft, Phys. Rev. Lett. **21**, 1748 (1968); T. Schneider, Helv. Phys. Acta **42**, 957 (1969); L. G. Caron, Phys. Rev. B **9**, 5025 (1974); D. Papaconstantopoulos, L. L. Boyer, B. M. Klein, A. R. Williams, V. L. Morruzzi, and J. F. Janak, *ibid.* **15**, 4221 (1977); A. C. Switendick, in *Superconductivity in d- and f-Band Metals,* edited by D. H. Douglass (Plenum, New York, 1976), p. 593; D. A. Papaconstantopoulos and B. M. Klein, Ferroelectrics **16**, 307 (1977); B. I. Min, H. J. F. Jansen, and A. J. Freeman, Phys. Rev. B **33**, 6383 (1986).

[3]R. J. Miller and C. B. Satterthwaite, Phys. Rev. Lett. **34**, 144 (1975).

[4]A. W. Overhauser, Phys. Rev. B **35**, 411 (1987).

[5]N. A. Bell and G. E. Coates, J. Chem. Soc. A **1968**, 628 (1968).

[6]A. C. Switendick, Z. Phys. Chem. Neue Folge **117**, 89 (1979).

[7]B. K. Rao and P. Jena, Phys. Rev. B **31**, 6726 (1985).

[8]W. J. Hehre, L. Radom, P. v. R. Schleyer, and J. A. Pople, *Ab Initio Molecular Orbital Theory* (Wiley, New York, 1986).

[9]W. J. Hehre, R. Ditchfield, and J. A. Pople, J. Chem. Phys. **56**, 2257 (1972).

[10]P. Hohenberg and W. Kohn, Phys. Rev. **136**, B864 (1964); W. Kohn and L. J. Sham, *ibid.* **140**, A1133 (1965).

[11]E. J. Baerends, D. E. Ellis, and P. Ros, Chem. Phys. **2**, 41 (1973); D. E. Eillis and G. S. Panter, Phys. Rev. B **2**, 2887 (1970); D. E. Ellis, G. A. Benesh, and E. Byrom, *ibid.* **16**, 3308 (1977).
[12]B. K. Rao and P. Jena, Phys. Rev. B **32**, 2058 (1985).
[13]L. Hedin and B. I. Lundqvist, J. Phys. C **4**, 2064 (1971); U. von Barth and L. Hedin, J. Phys. C **5**, 1629 (1972).
[14]B. K. Rao and P. Jena, J. Phys. C **19**, 5167 (1986).
[15]V. L. Moruzzi, J. F. Janak, and A. R. Williams, *Calculated Electronic Properties of Metals* (Pergamon, New York, 1978).
[16]W. Y. Ching, Y. Xu, G. L. Zhao, K. W. Wong, and F. Zandiehnadem, Phys. Rev. Lett. **59**, 1333 (1987).